A coupled numerical approach for assessing the bearing capacity of an eccentrically loaded foundation on layered cohesionless soil near a slope

Rajib Dey
Stantec Consulting Ltd., Markham, Ontario, Canada
Muhammad Abdur Rahman & Naveel Islam
Military Institute of Science and Technology (MIST), Dhaka, Bangladesh

ABSTRACT
Bearing capacity of shallow foundations near slopes and embankments are commonly assessed in geotechnical practice. Few studies are available in the literature that assess the bearing capacity for an eccentrically loaded footing located adjacent to a cohesionless soil slope. In some instances, this problem is further complicated due to the presence of layered soils located near a slope and the possibility of punching shear failure. This problem is not well understood and there is little design guidance published for the practicing geotechnical engineers. The authors have previously completed finite difference analyses to model the failure mechanisms of a vertically loaded strip footing on layered dense over loose cohesionless soils near a slope. In this study, the authors have extended their assessment of this problem by introducing eccentric loading to the aforementioned problem. This paper presents an overview of the numerical modeling methodology, results of the analysis, and presents design considerations.

RÉSUMÉ
La capacité portante des fondations peu profondes près des pentes et des remblais est généralement évaluée dans le cadre de la pratique géotechnique. Il existe peu d'études dans la littérature qui évaluent la capacité portante d'une semelle chargée de manière excentrée située à proximité d'une pente de sol sans cohésion. Dans certains cas, ce problème est encore compliqué par la présence de sols stratifiés situés près d'une pente et par la possibilité d'une rupture par poinçonnement. Ce problème n'est pas bien compris et il existe peu de directives de conception publiées pour les ingénieurs géotechniciens en exercice. Les auteurs ont précédemment réalisé des analyses par différences finies pour modéliser les mécanismes de défaillance d'une semelle filante chargée verticalement sur des sols denses en couches sur des sols non cohésifs lâches à proximité d'une pente. Dans cette étude, les auteurs ont étendu leur évaluation de ce problème en introduisant une charge excentrique au problème susmentionné. Cet article présente une vue d'ensemble de la méthodologie de modélisation numérique, des résultats de l'analyse et présente des considérations de conception.

1 INTRODUCTION

Structures are often constructed near slopes, requiring a bearing capacity assessment of the layered subsurface soils beneath the structure. In the literature, the bearing capacity of foundations under uniform loading near a homogeneous slope has been well studied (Meyerhof, 1957; Shields et al, 1977; Andrews, 1986; Graham et al, 1987; Tatsuka, et al, 1987; Gemperline, 1988; Garnier et al, 1994). The punching shear failure of footings on a horizontal ground surface has also been widely studied and published in the literature (Button, 1953; Reddy and Srinivasan, 1967; Brown and Meyerhof, 1969; Meyerhof, 1974; Meyerhof and Hanna, 1978; Hanna and Meyerhof, 1979, 1980, 1981; Hanna, 1981a, 1981b, 1982). Although comprehensive research has been completed for both these problems independently, the authors did not find any direct study in the literature assessing the failure mechanisms associated with the bearing capacity failure of an eccentrically loaded footing on layered soils near a slope. It is noted that authors completed a study (Dey et al, 2016) to assess the failure mechanisms of a strip footing founded on a dense sand layer overlying a loose sand layer near a slope; however, eccentric loading was not considered in that study.

Turker et al. (2014) completed a study to determine the bearing capacity of eccentrically loaded strip footings close to a geotextile-reinforced homogenous sand slope. A series of physical and laboratory tests were conducted to determine the bearing capacity of footing for various eccentricity. Zerguine et al. (2018) completed numerical modeling to determine the bearing capacity and behaviour of an eccentrically loaded strip footings adjacent to a cohesionless slope. Mansouri and Abbeche (2019) also completed an experimental study to determine the bearing capacity of an eccentrically loaded foundation near a slope. Since there is no specific design method available for such footings, these recent studies provide advancement to the specific problem. However, none of these studies consider a layered soil system.

This paper presents results of numerical analysis which assessed the failure mechanisms of an eccentrically loaded strip footing founded on a dense sand layer overlying a loose sand layer near a slope. The assessment consisted of a parametric study to explore the relationship of footing size to upper dense layer thickness, depth of footing, slope angle, and the effect of footing offset from the edge of the slope. A study was also carried out comparing the results to traditional methods used to estimate the ultimate capacity of an eccentrically loaded footing on layered soil near a slope.

2 PROBLEM DEFINITION

Figure 1 shows the geometry of a two-layered soil system considered in this study.

In order to validate the finite element model developed in the present research, analysis was first completed considering a strip footing (width, *B*) placed on a level ground on a layered cohesionless soil (Fig. 1a). The footing depth was defined as D_f and the thickness of a loose sand layer below dense sand layer was considered as *h*. The thickness of the dense sand layer below the footing was assumed as *y*. A vertical eccentric load, *P* was applied at a distance, *e* = 0.15 m (e <B/6) from the center line towards the left side of the foundation (Fig. 1a). When the footing is subjected to a large vertical eccentric load, a punching failure will occur depending on the thickness of the dense sand layer below the footing. The ultimate bearing capacity of this eccentrically loaded footing can be estimated based on the solutions available in the literature.

The problem is further analyzed assuming the footing placed at a distance *x* from the crest of a slope (Fig. 1 b).

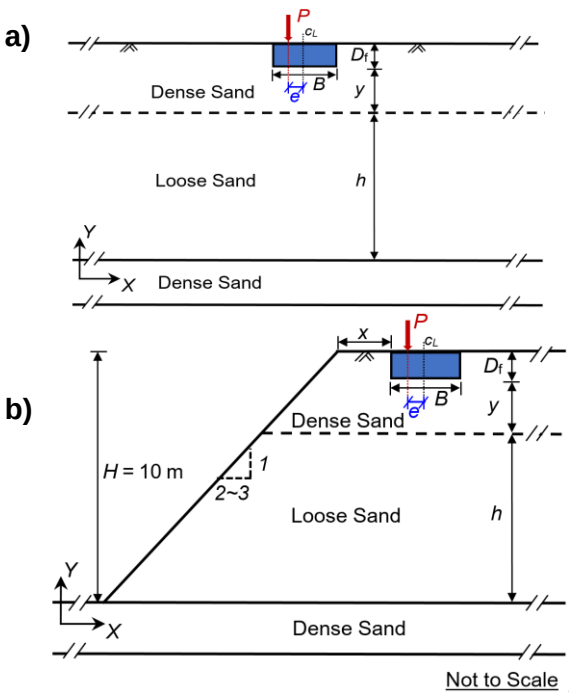

Fig 1. Geometry of the problem: a) footing on level ground, and b) footing near slope

For both problems, *B* = 1 m, D_f = 0 and *y* = 1 m are assumed for the base case model. A value of *h* = 14 m (Fig. 1a) and *h* = 9 m (Fig. 1b) are considered for level ground and sloping ground, respectively. From the crest of a 2H:1V slope (slope angle, β = 26.6°) a footing distance of *x* = 1 m was maintained. Analyses were conducted in this study varying the values of *x*, *y*, D_f and β (changing one parameter at time). The soil boundary was extended sufficiently in the lateral direction (60 m) and along the depth (20 m) to avoid any boundary effects on stability and potential failure mechanisms. For simplicity, groundwater table is not considered in the study. Hence, there is no generation of excess pore water pressure.

To show the effects of a slope on the ultimate bearing capacity of an eccentrically loaded footing near a slope on layered soil, a percentage reduction on capacity is presented based on the ratio between the ultimate bearing capacity obtained from Fig. 1b and the ultimate bearing capacity from Fig. 1a. This approach is similar to the percentage of capacity charts (for vertical concentric loads) presented by Shields et al. (1990).

3 FINITE ELEMENT MODELING

3.1 Numerical Technique

For the numerical analyses, finite element (FE) program, PLAXIS 2D (version 2018.01) is used following the implicit solution scheme. The implict scheme of Newmark is a frequently used method in FE analyses which generally produces a more stable calculation process and a more accurate soultion (Sluys, 1992). As per Vermeer (1979), the implicit scheme leads to a symmetic and positive differential matrix that accelerates the iteration processes.

For higher accuracy, a 15-noded triangular elements in plain strain condition is considered. The global mesh generation technique with enhanced mesh refinement formulation is considered. In PLAXIS 2D, the mesh generator requires a global meshing parameter that represents a target element size or an average element size, l_e. This target element dimension changes with the shape of the model geometry and a relative element size factor, r_e (i.e. for element distribution of very fine mesh, the value of r_e = 0.50 and very coarse mesh, the value of r_e = 2.00). Appropiate interface elements (available in Plaxis) are also used in between the dense sand and footing surface.

Roller supports are used for the left and right vertical faces, while at the bottom face hinge supports are used.

3.2 Loading Steps

The FE analyses generally consists of two loading steps. At first, the gravity loading was applied to bring the soil to in-situ stress conditions. At the end of attainment of initial stresses, the incurred displacements were reset to zero before the next step of analysis. In the second step, the external vertical eccentric point load, P was applied gradually at a distance of *e* from the c_L of the footing until the failure occurred (Fig. 1). In the program, the difference between the total of internal stresses and any of the external applied load was termed as *unbalance*, and denoted by $\sum M_{stage}$ multiplier. $\sum M_{stage}$ = 0, indicates that unbalance is not solved whereas $\sum M_{stage}$ = 1, denotes full unbalance has been solved. Hence, the ultimate capacity (pressure underneath the footing) of a foundation can be determined from the summation of the stresses developed in the insitu stage and the percentage of the change of load developed in the $\sum M_{stage}$ multiplier for the externally applied load.

Additionally, the safety calculations were also adopted to determine the Factor of Safety (FOS) using the strength reduction method (Cheng et al. 2007; Griffiths and Lane

1999; Griffiths and Marquez 2007; Saha et al 2014). In the program, the safety calculations were made in terms of the multiplier denoted by $\sum M_{sf}$. Initially, the value of $\sum M_{sf}$ was set to 1.0, representing all the soil parameters to their input values. At the end of each loading step, the strength parameters of the soil were successively reduced until failure at the interface of the soil-structure occurred. Hence, the value of $\sum M_{sf}$ at failure denotes the value of FOS at that loading stage.

When the footing was placed at a depth of D_f below the ground level, there is an effect of overburden pressure. In that case, an additional loading step was created before applying the load on the footing (second step) where pressure equivalent to depth of overburden was applied on the ground surface. This simulates the effect of overburden stress at depth D_f. Load on the footing (P) was then applied in the following steps as mentioned earlier.

3.3 Modeling of Soil and Structure

The soil was modeled as linear elastic-perfectly plastic material using the Mohr–Coulomb yield criterion. A constant average stiffness was assumed for each layer. The base of the strip footing was defined in the form of a linear elastic non-porous plate. In the program, the weight of the plate was considered along with the weight of the soil by means of the $\sum M_{weight}$ parameter. The material parameters used in the analyses, are shown in Table 1.

Table 1. Material Parameters

Parameters	Values		
	Dense Sand	Loose Sand	Concrete Footing
Young's modulus, E' (MPa)	50	10	20x 10^3
Poisson's ratio, ν'	0.3	0.3	0.20
Angle of internal friction, ϕ' (°)	35	30	-
Unit weight, γ' (kN/m^3)	21	19	24

4 RESULTS

4.1 Validation of the numerical model

The problem presented in Fig. 1a was analyzed first and the results obtained from FE model are validated with the ultimate capacity calculated using available solutions (Hanna, 1981a). Fig. 2 shows the results obtained from the PLAXIS 2D analysis.

The solid blue line in Fig. 2 shows the change of applied pressure with displacement. The blue dashed line with diamond bullets represents the variation of applied pressure (due to the eccentric load at the top of the foundation) against the factor of safety (FOS). Before the application of the load, an initial pressure of 10 kPa was applied to simulate the weight of the footing which results a FOS equals to 3.25. The graph indicates that FOS drops from 3.25 to 1.0 when applied load is increased from 10 to 195 kPa. Hence, the model fails at 195 kPa when the FOS ≤ 1. A punching shear failure occurs in the dense sand layer, followed by a general shear failure in the loose sand layer as shown in Fig. 3.

To check the effect of mesh size, analyses were conducted for different relative element size factors (r_e). As observed (from Fig 2), the pressure vs displacement plot for r_e = 0.5 coincides with the pressure vs FOS plot. However, analyses for the higher r_e values (Fig. 3a-c) over predicts the capacity and the associated total displacement. Hence, as a reasonable estimate all the following analyses discussed in the later part of this study was conducted considering a r_e = 0.5 (*very fine mesh*).

The ultimate capacity calculated from available solutions (Hanna, 1981a condidering the effect of eccentricity) is 198 kPa and is shown by the vertical dashed line in Fig. 2. The ultimate capacity of the footing estimated from the numerical analysis matches well with available solutions. The modeling technique used in this case is further utilized to model the problem mentioned in Fig.1b.

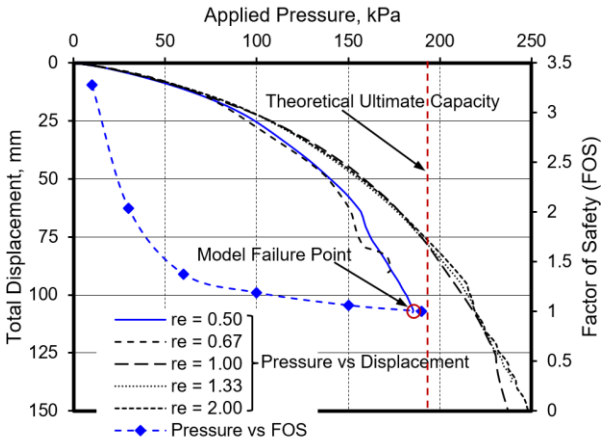

Fig 2. Validation of the FE model

4.2 Calculation of Ultimate Capacity

The problem shown in Fig. 1b is used to estimate the ultimate capacity of an eccentrically loaded footing on layered soil near a slope. A base model is considered first assuming a 2H:1V slope as mentioned in Section 2. The numerical model is also validated with Shield's method, widely used for calculating bearing capacity of a concentrically loaded foundations in slopes assuming homogenous foundation materials.

A percentage reduction on ultimate capacity can be determined comparing the ultimate capacity obtained for the problem mentioned in Fig. 1b (*UC*) with the ultimate capacity of a reference footing on level ground as mentioned in Fig. 1a (UC_{ref}). The ultimate capacity, UC_{ref}, can be calculated using equations proposed by Hanna, 1981a incorporating the effect of eccentric loading using Meyerhof's (1953) effective width concept (e.g. using B' = B – 2e instead of B). The ratio of these two ultimate capacities can be expressed in percentage using a term called "reduction factor (R_{uc})" and is defined as:

$$R_{uc} = UC / UC_{ref} \times 100\% \quad [3]$$

For example, a value of R_{uc} = 42.9% can be obtained for the base case model where UC_{ref} = 196 kPa and *UC* = 84 kPa. Therefore, the ultimate capacity of an eccentrically

loaded footing supported by dense sand layer underlain by a loose sand layer is reduced by approximately 57% when the footing is placed at 1 m distance from the crest of the slope. In other words, if the ultimate capacity of the reference footing under eccentric load (UC_{ref}) can be calculated using Hanna's equations (condidering the effect of eccentricity), then the ultimate capacity of the footing shown in Fig. 1b can be estimated by multiplying UC_{ref} by R_{uc}.

3 PARAMETRIC STUDY

For the eccentrically loaded footing near slope model (Fig 1b), base case model was used to perform a parametric study. Values of D_f/B are varied from 0 to 1, x/B are varied from 0 to 2 and y/B are varied from 1 to 2 in order to capture the effect of depth of footing, footing distance from the crest of the slope, and depth of the dense sand layer. Analyses were conducted to determine the ultimate capacity of foundation considering a 2H:1V and 3H:1V slopes. Reduction factor (R_{uc}) has been determined for each case by changing one variable at a time. The results obtained from the analyses are presented in Figs. 4–9.

4.1.1 Effect of *y*/B

Figures 4 and 5 show the total displacement contour plot for 2H:1V and 3H:1V slopes respectively varying the thickness of upper dense sand layer (y) underneath the foundation. All the analyses were completed for x =1 m, D_f =0 and h = 9 m. The results indicate that the magnitude of y in Fig. 1 has a significant importance on ultimate bearing capacity as well as on the failure mechanisms. For example, if the value of y is relatively large, the failure pattern will change from a punching shear failure to a general bearing capacity failure for a level ground. However, this might not be always the case if the footing is placed near the crest of the slope as shown in Fig. 1b. Plastic shear strain is generated along the failure plane and the failure surfaces propagate through the loose layer for all cases. This shows that there is a tendency of forming a combined punching/bearing capacity and deep-seated failure surface when y increases. However, the tendency of the global slope failure decreases for a relatively flat (3H:1V) slope when *y*/B increases.

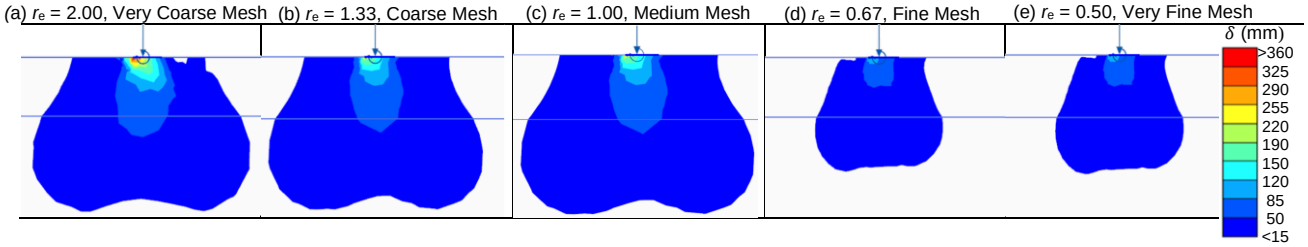

Fig 3 Failure Surface for mesh size (Level Ground)

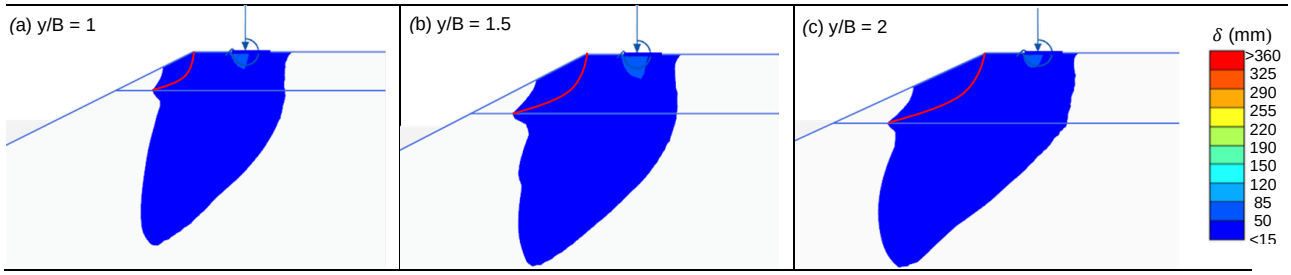

Figure 4 Slope failure due to eccentric load for footing placed at x =1 m for different *y*/B (2H:1V slope)

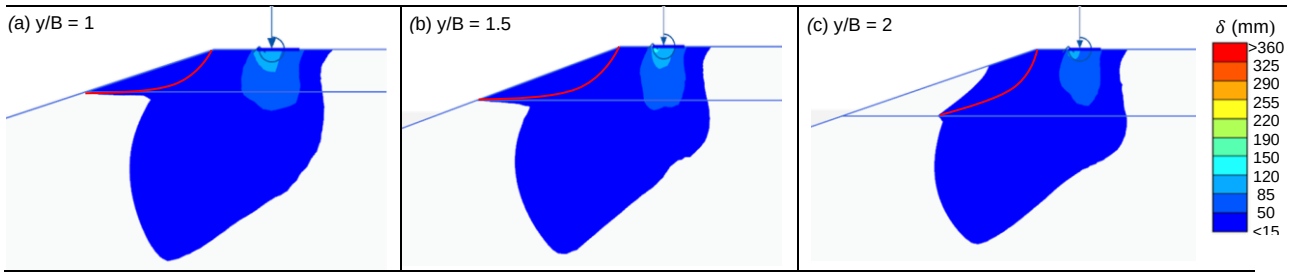

Figure 5: Slope failure due to eccentric load for footing placed at x =1 m for different y/B (3H:1V slope)

4.1.2 Effect of D_f/B

Figure 6 and 7 show the variation of D_f/B against a reduction factor, R_{UC} in percentages for the problem mentioned in Figure 1b. Analyses were completed varying y/B = 1 to 2, and increasing the value of D_f from 0 to 1 for eccentricity, e = 0.15 m. The results indicate that the values of R_{UC} are smaller when depth of the footing (D_f) increases. This is due to the fact that UC_{ref} increases significantly with increasing of D_f, but the value of UC increases slightly when the value of D_f increases. That means, although the depth of the footing has a significant contribution on ultimate capacity calculation of an eccentrically loaded footing placed on level ground, the effect is relatively small on slope capacity calculation when the footing is placed on a layered soil and adjacent to a slope. Therefore, a smaller value of R_{uc} results with an increase in D_f /B as shown in Figs. 6 and 7.

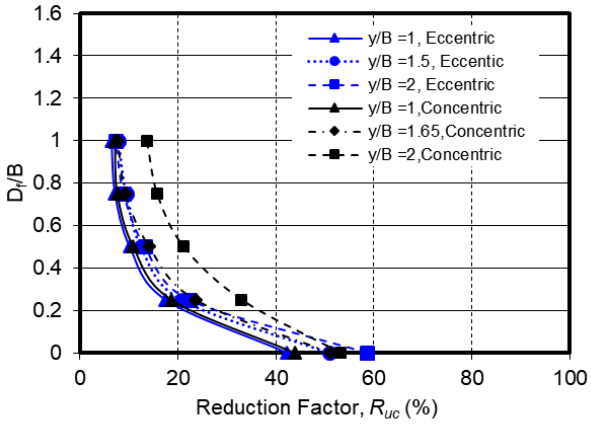

Fig 6 Variation of D_f/B with R_{UC} for 2H:1V slope

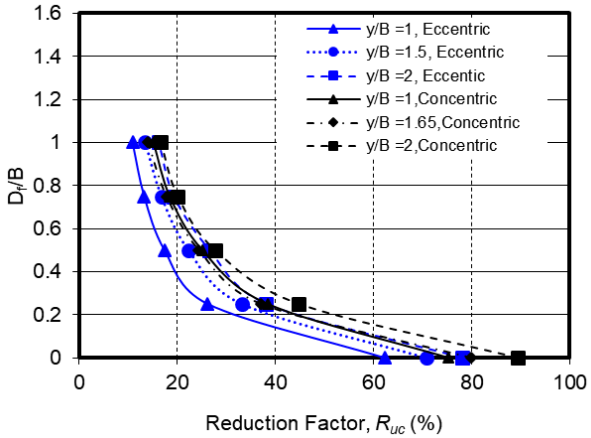

Fig 7 Variation of D_f/B with R_{UC} for 3H:1V slope

For example, if the footing is placed at ground surface (D_f = 0) and y/B=1, the reduction factor will be 38% while estimating the ultimate capacity of the eccentrically loaded footing. That means, if UC_{ref} can be calculated using available solutions, the ultimate capacity of the footing for this scenario will be 38% of UC_{ref}. For a 3H:1V slope, the value of R_{UC} is greater than the values obtained for 2H:1V (compare Figure 6 and 7). Similar trend can be obtained for concentric loading (see Figure 6 and 7); however the capacity will be smaller for the eccentric loading condition.

4.1.3 Effect of x/B

Figures 8 and 9 show the variation of x/B with R_{UC} for two different slope angles. Analyses were completed for D_f =0 and increasing the value of x from 0 to 1 and varying y/B = 1 to 2 for eccentricity, e = 0.15 m. The results indicate that the distance of footing from the slope crest (x) has also a significant influence on slope ultimate capacity (UC). As x increases, UC increases. However, in this case UC_{ref} remains constant as UC increases, which results in an increasing value of R_{uc}. This trend (increase of R_{UC} with x/B and y/B) continues regardless of the slope angle considered in this study. Similar trends are also observed for concentric loads (see Figure 8 & 9), however the capacity will be smaller for the eccentric loading condition.

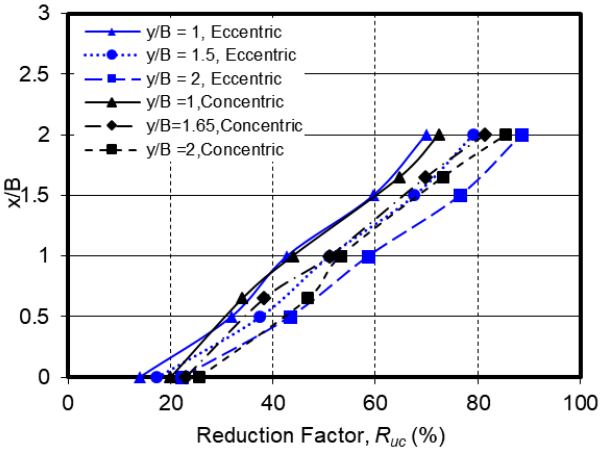

Fig 8 Variation of x/B with R_{UC} for 2H:1V slope

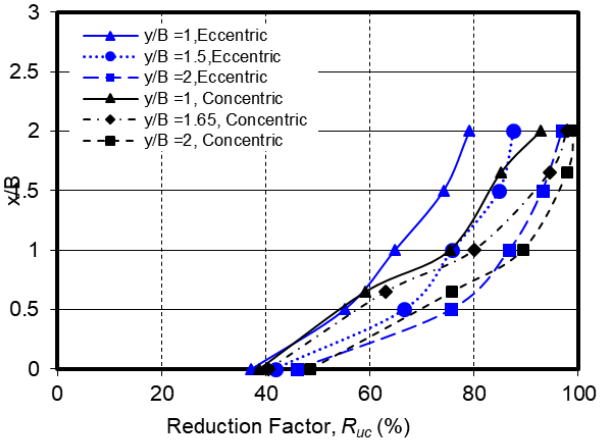

Fig 9 Variation of x/B with R_{UC} for 3H:1V slope

5 COMPARISON WITH UNCOUPLED APPROACH

In uncoupled approach, the calculations for the ultimate capacity for a sloping ground is estimated in two separate stages. Firstly, the ultimate bearing capacity for an eccentrically loaded footing can be estimated using the analytical calculation (Hanna's (1981) method) scheme for a level ground incorporating the effect of eccentric loading using Meyerhof's (1953) effective width concept. Then the calculated ultimate capacity is reduced using Shields et al. (1990) reduction factors (percent capacity charts) to incorporate the slope geometry. Therefore, the final ultimate capacity can be calculated using an uncoupled approach. These methods have been used and accepted for their intended design; however, this uncoupled approach may underestimate or overestimate the footing capacity since these methods were not originally developed for addressing the problem (Fig. 1b) presented in this study. Whereas in a coupled approach, using the modern geotechnical analyses tool (e.g. advanced numerical techniques) a better control on the complex boundary problems could be attained. This might better predict the actual capacity of an eccentrically loaded footing near a slope.

In the following sections, a comparison is made between the coupled and uncoupled approach for the problem mentioned in Figure 1(b) varying the depth of the foundation, slope angles and crest distances. The difference between the percentage of the ultimate capacity ratio is expressed in the form, $\Delta = (1- UC/UC_{uncoupled}) * 100$ (%); where, $UC_{uncoupled}$ is the ultimate capacity estimated using the uncoupled approach.

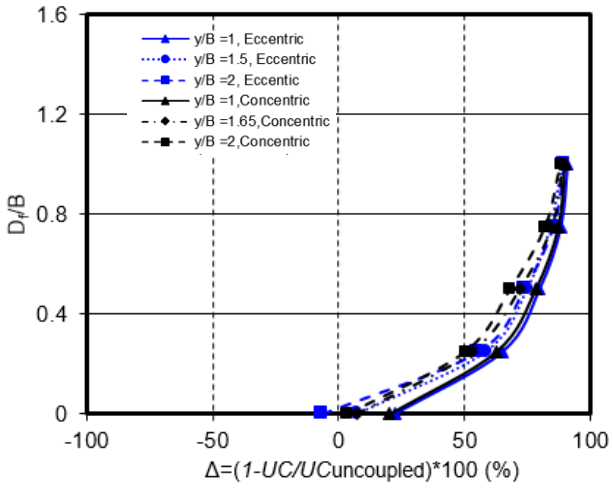

Fig 10: Ultimate capacity comparison with uncoupled approach for 2H:1V slope for D_f/B

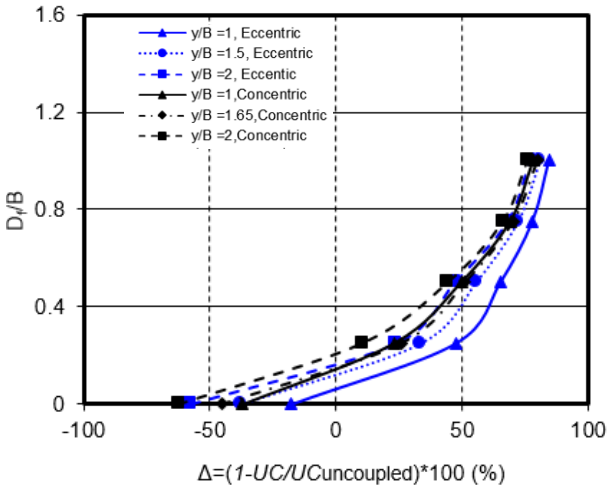

Fig 11: Ultimate capacity comparison with uncoupled approach for 3H:1V slope for D_f/B

5.1 Comparison for D_f/B

Figure 10 and 11 show the variation of D_f/B with Δ, for 2H:1V and 3H:1V slopes respectively for different values of *y*/B. The results indicate that the difference between coupled and uncoupled approach gradually increase with the increase in footing depth. The uncoupled approach over predicts the capacity.

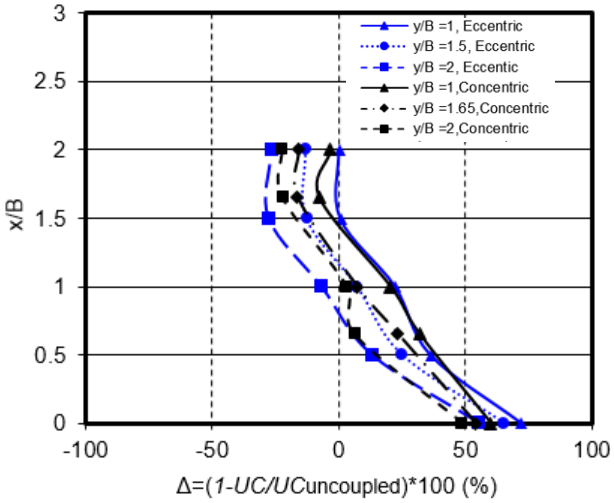

Fig 12: Ultimate capacity comparison with uncoupled approach for 2H:1V slope for *x*/B

5.2 Comparison for x/B

Figures 12 and 13 present the variation of *x*/B with Δ, for 2H:1V and 3H:1V slopes respectively for different values of *y*/B. The results indicate that the uncoupled approach under predicts the capacity with the increase in the distance of the foundation from the crest of the slope.

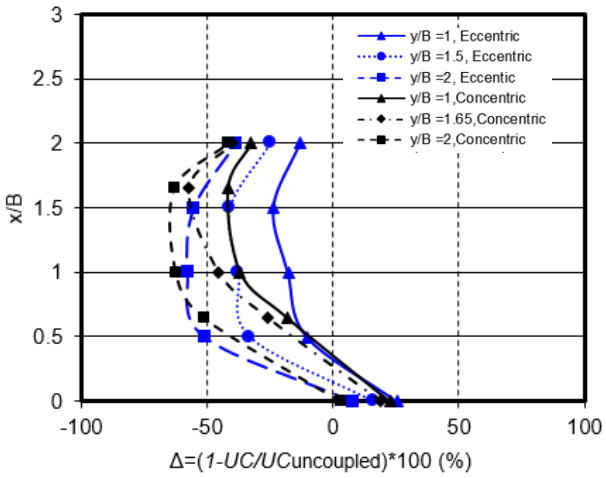

Fig 13: Ultimate capacity comparison with uncoupled approach for 3H:1V slope for *x*/B

6 CONCLUSIONS

The following conclusions can be drawn from this study:

- The thickness of the upper dense soil layer beneath the footing (*y*) significantly influences ultimate capacity (*UC*) of footings on layered soils. It is shown that *UC* increases with increase in *y* for both concentric and eccentric conditons; however, UC will be samller for eccentric conditions.
- With increase of distance of the footing from the slope crest (*x*), *UC* increases for both conditions. For a large value of *x*, punching failure will govern instead of global slope failure.
- Unexpectedly, the value of R_{uc} decreases with increasing depth of the footing (D_f). As the footing is placed at only 1 m distance from the crest of the slope, the global slope capacity remains almost constant for these analyses. Slope failure occurred through the loose layer for all cases. The ultimate capacity will be samller for eccentric loading conditions.
- Practical design application of these data are limited to only B = 1 for concentric load (e = 0 m) and B' = 0.7 for eccentric load (e = 0.15 m).
- Practicing engineers should use uncoupled approach with caution for both concentric and eccentric loading conditions.
- In practice, the coupled approach should be used as it captures the actual combined punching shear and slope failure mechanisms.

Further research is required to assess the effect of distance of vertically applied eccentric load from the center line of the footing (various eccentricity) on bearing capacity of foundation placed on layered cohesionless soil near slope, and produce design charts and methodology.

7 ACKNOWLEDGEMENTS

The authors would like to express their sincere gratitude to Geomechanics Lab of Military Institute of Science and Technology (MIST), Bangladesh for their financial and licensing supports.

REFERENCES

Andrew, M. 1986. Computation of bearing capacity coefficients for shallow footings on cohesionless slopes using stress characteristics, M.Sc. Thesis, University of Manitoba, Manitoba.

Brown, J. D. and Meyerhof, G. G. 1969. Experimental Study of Bearing Capacity in Layered Clays, *Proceedings of the* 7th *International Conference on Soil Mechanics and Foundation Engineering,* Mexico, 2: 45-51.

Button, S. J. 1953. The Bearing Capacity of Footing on Two-Layer Cohesive Subsoil, *Proceedings of the 3rd International Conference on Soil Mechanics on Foundation Engineering,* 1:332-335.

Cheng, Y. M., Lansivaara, T., & Wei, W. B. 2007. Two-dimensional slope stability analysis by limit equilibrium and strength reduction methods. *Computers and geotechnics*, *34*(3), 137-150.

Dey, R., Parsons, S. and Stein, L. 2016. Bearing capacity of a foundation on layered soils near a slope - numerical analysis assessing punching shear failure and slope stability, *Canadian Annual Geotechnical Conference*, *GeoVancouver* 2016.

Garnier, J., Canepa, Y., Corte, J.F. and Bakir, N.E. 1994. Etude de la Portance de Foundations en Bord de Talus, *Proceedings of the 13th International Conference on Soil Mechanics and Foundation Engineering,* 2:705-708.

Graham, J., Andrews, M. and Sheilds, D.H. 1987. Stress Characteristics for Shallow Footings in Cohesionless Slopes, *Canadian Geotechnical Journal,* 25(2): 238-249.

Griffiths, D. V., & Lane, P. A. 1999. Slope stability analysis by finite elements. *Geotechnique*, *49*(3), 387-403.

Griffiths, D. V., & Marquez, R. M. 2007. Three-dimensional slope stability analysis by elasto-plastic finite elements. *Geotechnique*, *57*(6), 537-546.

Hanna, A. M., & Meyerhof, G. G. 1979. Ultimate bearing capacity of foundations on a three-layer soil, with special reference to layered sand. *Canadian Geotechnical Journal*, 16(2), 412-414.

Hanna, A. M. and Meyerhof G. G. 1980. Design Charts for Ultimate Bearing Capacity of Foundations on Sand Overlying Soft Clay, *Canadian Geotechnical Journal,* 17(2): 300-303.

Hanna, A. M. and Meyerhof G. G. 1981. Experimental Evaluation of Bearing Capacity of Footings Subjected to Inclined Loads, *Canadian Geotechnical Journal,* 18(4): 599-603.

Hanna, A.M. 1981a. Foundations on Strong Sand Overlying Weak Sand, *Journal of Geotechnical Engineering,* ASCE, 107(7): 915-927.

Hanna, A. M. 1981b. Experimental Study on Footings in Layered Soil, *Journal of Geotechnical Engineering,* ASCE, 107(8): 1113-1127.

Hanna, A. M. 1982. Bearing Capacity of Foundations on a Weak Sand Layer Overlying a Strong Deposit, *Canadian Geotechnical Journal,* 19(3): 392–396.

Mansouri, T., & Abbeche, K. 2019. Experimental bearing capacity of eccentrically loaded foundation near a slope. *Studia Geotechnica et Mechanica*, *41*(1), 33-41.

Meyerhof, G.G. 1957. The Ultimate Bearing Capacity of Foundation on Slopes, *Proceedings of the 4th International Conference on Soil Mechanics and Foundation Engineering,* 3: 384-386.

Meyerhof, G. G. 1974. Ultimate Bearing Capacity of Footings on Sand Layer Overlying Clay, *Canadian Geotechnical Journal,* 11: 223-229.

Meyerhof, G.G. and Hanna, A.M. 1978. Ultimate Bearing Capacity of Foundations on Layered Soils under Inclined Load, *Canadian Geotechnical Journal*, 15(4): 565-572.

Reddy, A. S. and Srinivasan R. J. 1967. Bearing Capacity of Footings on Layered Clays, *Journal of the Soil Mechanics and Foundations Division,* ASCE, 96(9): 1951-1965.

Saha, B., Hawlader, B., Dey, R. and McAffee, R. 2014. Slope Stability Analysis using a Large Deformation Finite Element Modeling Technique, *the 67th Canadian Geotechnical Conf.* – GeoRegina, Saskatchewan.

Shields, D.H., Scott, J.D., Bauer, G.E., Deschemes, J.H. and Barsvary, A.K. 1977. Bearing Capacity of Foundations Near Slopes, *Proceedings of the 9th International Conference on Soil Mechanics and Foundation Engineering,* 1: 715-720.

Shields, D., Chandler, N. and Garnier J. 1990. Bearing Capacity of Foundations In Slopes, *Journal of Geotechnical Engineering,* ASCE, *116*(3): paper No. 24482.

Sluys, L. J., & De Borst, R. 1992. Wave propagation and localization in a rate-dependent cracked medium—model formulation and one-dimensional examples. *International Journal of Solids and Structures*, *29*(23), 2945-2958.

Turker, E., Sadoglu, E., Cure, E., & Uzuner, B. A. 2014. Bearing capacity of eccentrically loaded strip footings close to geotextile-reinforced sand slope. *Canadian Geotechnical Journal*, *51*(8), 884-895.

Vermeer, P. A. 1979. A modified initial strain method for plasticity problems. In *Proc. 3rd Int. Conf. Num. Meth. Geomech. Balkema, Rotterdam* (pp. 377-387).

Zerguine, S., Benmeddour, D., Ouahab, M. Y., Mabrouki, A., & Mellas, M. 2017. Bearing capacity of eccentrically loaded strip footings near a slope. In *Global Civil Engineering Conference* (pp. 1285-1293). Springer, Singapore.